Sequential ^{1}H NMR Assignment of the Complex of Aponeocarzinostatin with Ethidium Bromide and Investigation of Protein–Drug Interactions in the Chromophore Binding Site†

Smita Mohanty,‡ Larry C. Sieker,§ and Gary P. Drobny*,‡

Departments of Chemistry and Biological Structure, University of Washington, Seattle, Washington 98195

Received December 28, 1993; Revised Manuscript Received May 16, 1994®

ABSTRACT: Two-dimensional ^{1}H NMR spectroscopy has been used to investigate the binding site, binding interactions, and the conformation of a 1:1 complex of aponeocarzinostatin (apo-NCS) with ethidium bromide in solution. The protein component in the complex has been sequence-specifically assigned using information derived from coherence transfer and two-dimensional homonuclear ^{1}H NOESY experiments. The conformation of the protein in the complex has been found to be similar to the free form of the apoprotein, and intermolecular NOEs between the residues of the protein to protons on the ethidium bromide suggest that the ethidium bromide is bound to the protein in the same cleft in which the neocarzinostatin chromophore binds. Protons on ethidium show NOE interactions to the following protein residues: Trp-39, Leu-45, Cys-47, and Gln-94 which interact with the phenanthridine ring system of ethidium, Gly-102 and Asn-103 which interact with the alkyl chain of ethidium, and Phe-52 which interacts with the phenyl ring of ethidium. The orientation of ethidium in the cleft of apo-NCS is compared and contrasted to orientation of the chromophore as determined by high-resolution NMR and X-ray diffraction studies.

Neocarzinostatin (NCS)[1] is a DNA-nicking protein antibiotic isolated from the culture broth of *Streptomyces carzinostaticus* (Ishida et al., 1965). It is a prominent member of the Streptomyces family of macromolecular antitumor antibiotics that includes actinoxanthin (AXN) and auromomycin (AUR). NCS has attracted great interest and is the best studied of the Streptomyces anticancer agents. NCS has a relatively low toxicity (LD_{50} of 10–30 mg/kg in mice and dogs) and a broad in vivo activity against human leukemia, bladder cancer, liver metastasis, and sarcoma (Montgomery et al., 1981). The NCS holoprotein (holo-NCS) and consists of a fluorescent chromophore (NCS-Chr) of molecular weight 659, which is tightly, but noncovalently bound to a 11 100-Da protein (apo-NCS). The inhibition of cell growth by this drug has been attributed to its nonprotein chromophore, which causes DNA strand scissions through radical reactions (Kappen et al., 1982, 1989; Favaudon et al., 1985; Kappen & Goldberg, 1993). The chromophore (see Figure 1a) is very sensitive to heat, light, and molecular oxygen and is easily inactivated due to its labile and reactive molecular structure, which contains both epoxy and acetylenic functions (Goldberg et al., 1981). Despite its intrinsic instability in the free state, the chromophore is relatively stable in the complex with the protein. Apo-NCS has no demonstrated cytotoxic activity and is believed to primarily serve as a carrier, protecting the chromophore from decomposition. There is some evidence suggesting that, upon penetration into the cell, NCS releases the active principle at the level of the cell nucleus, which then exerts its pharmacological activity (Maeda et al., 1975; Takeshita et al., 1980).

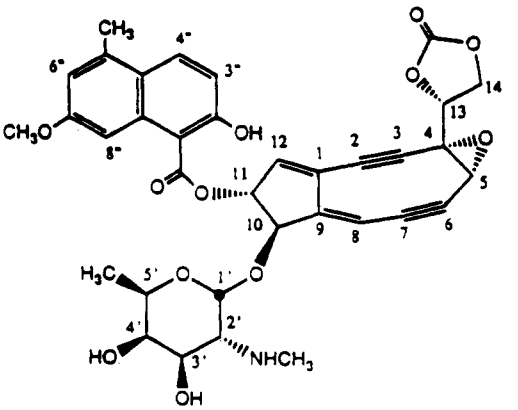

FIGURE 1: (a) Chemical structure of neocarzinostatin chromophore (NCS-Chr). (b) Chemical structure of ethidium bromide.

Both AXN and AUR have about 50% sequence homology with NCS (Khokholov et al., 1976; Samy et al., 1983) and possess nonprotein chromophores. Results of X-ray studies

† This research was supported by NIH Grant RO1 CA45643-03.

‡ Department of Chemistry.

§ Department of Biological Structure.

® Abstract published in *Advance ACS Abstracts,* July 15, 1994.

[1] Abbreviations: NMR, nuclear magnetic resonance; NCS, neocarzinostatin; Chr, chromophore; AUR, auromomycin; AXN, actinoxanthin; 2D, two dimensional; COSY, 2D correlated spectroscopy; DQF, double quantum filtered; TQF, triple quantum filtered; RELAY, 2D relayed coherence transfer spectroscopy; TOCSY, 2D total correlation spectroscopy; NOE, nuclear Overhauser effect; NOESY, 2D NOE spectroscopy; TPPI, time-proportional phase incrementation; ppm, parts per million; d_{AB}, the NOE connectivity between protons A and B of the same (intraresidue) or different (interresidue) amino acids in a polypeptide. Protons A and B are designated N for amide protons, α for CαH, β for CβH, etc.

0006-2960/94/0433-10579$04.50/0

confirm that NCS, AUR (Van Roey et al., 1989), and AXN (Pletnev et al., 1982) have similar overall structures as the degree of sequence homology would suggest and each protein has a well-defined binding cleft. The structure of AUR-Chr is only partially elucidated but is known to consist partly of a double ring system containing a benzoxazine carboxylate moiety instead of a naphthoic acid group (Kumada et al., 1983).

NCS-Chr and AUR-Chr both act by causing single- or double-strand breaks in DNA, but there are key differences in their mechanisms of action. The structure and the mechanism of action of NCS-Chr have been thoroughly studied (Edo et al., 1985; Myers et al., 1988; Meschwitz et al., 1992). The naphthoic moiety of NCS-Chr intercalates into DNA via the minor groove and causes strand scission of DNA, preferentially at thymidine or adenosine residues (Dasgupta et al., 1985; Takeshita et al., 1981). AUR exhibits a different site selectivity (guanidine and cytosine) for DNA strand scission (Takeshita et al., 1981; Kappen et al., 1979; Suzuki et al., 1980).

Kappen and Goldberg (1993) have recently reported site-specific cleavage at a DNA bulge by NCS-Chr via a novel mechanism. For single-stranded DNA to be cleaved by NCS-Chr, the DNA must generate a hairpin structure with an apical loop and at least a two-base-pair stem hinged to a region of duplex structure via a bulge containing a target nucleotide at its 3′ side.

The secondary and tertiary structure of apo-NCS is well understood from X-ray diffraction (Sieker, 1981) and NMR (Adjadj et al., 1990; Remerowski et al., 1990; Gao et al., 1991; Adjadj et al., 1992). An X-ray structure of the NCS holoprotein has been recently reported (Kim et al., 1993) as well as a model for the chromophore–protein complex based on a set of intermolecular NOEs (Tanaka et al., 1993).

Despite the sequence homology between NCS and AUR, apo-NCS does not bind AUR-Chr well nor does apo-AUR stabilize the NCS-Chr properly (Kappen et al., 1980; Kappen & Goldberg, 1980), so binding between NCS and its chromophore is to an extent specific. Unfortunately, the lack of information on the structure of AUR-Chr precludes comparative study by NMR or X-ray diffraction of the nature of drug–protein interactions in these systems.

However, in addition to binding NCS-Chr, it is known from X-ray studies that apo-NCS binds to a number of drugs including ethidium bromide (Figure 1b) and daunomycin (Sieker et al., unpublished results). We have therefore initiated a study by high-resolution solution NMR of the structures of these apo-NCS–drug complexes and have the goal of using the drug–protein interactions identified in these studies to better understand which structural features of a drug are vital in specifying binding to NCS. In this paper, we report the sequential assignment of the apo-NCS–ethidium bromide complex as well as the binding site and binding interactions of ethidium bromide to NCS. Ethidium bromide, like NCS-Chr, possesses a polyaromatic system and is a known DNA intercalator. It is also biologically active, possessing trypanocidal (Newton, 1964) and antiviral and antibacterial properties (Dikinson et al., 1953; Seaman et al., 1954; Vilagines et al., 1967). Like NCS-Chr, ethidium bromide inhibits DNA synthesis both in vivo (Henderson, 1963) and in vitro (Elliott, 1963; Waring, 1964).

A complete spectral assignment of the protons of apo-NCS in the complex with ethidium has enabled the identification of numerous protein–drug NOEs from which we have determined that ethidium binds in a 1:1 complex with NCS in the same cleft occupied by the NCS chromophore. The interactions of ethidium with amino acid residues in NCS are compared to the protein–chromophore interactions identified by NMR and X-ray diffraction.

MATERIALS AND METHODS

(a) Sample Preparation. The 1:1 apo-NCS–ethidium bromide complex was prepared by adding the protein solution into vials containing the drug. The final solution was purified by passing it through a Sephadex G-25 column followed by lyophilization. Apo-NCS was prepared from holo-NCS by extracting the chromophore using standard procedures (Napier et al., 1979). Purified, lyophilized holo-NCS was a gift from Kayaku Co. Ltd., Tokyo, Japan. Ethidium bromide was supplied by Sigma Chemical Co., St. Louis, MO.

For the detection of rapidly exchanging amide protons, the lyophilized complex was dissolved in 10 mM acetate buffer, pH = 5.0, and 10 mM EDTA in 0.5 mL of a mixed solvent of 90% H_2O/10% D_2O. The concentration was adjusted to between 2.0 and 2.5 mM for a 0.5-mL sample. For the identification of slowly exchanging amide protons, samples were lyophilized in NMR tubes and redissolved in 0.5 mL of 99.98% D_2O. Complete exchange of the labile protons with deuterium was obtained by keeping these solutions at 50 °C for 1 h, lyophilizing, and redissolving in D_2O.

(b) Fluorescence Measurements. Apo-NCS was dissolved in 10 mM sodium acetate, pH = 5.01. Relative fluorescence intensities of free ethidium bromide and the apo-NCS–ethidium bromide complex were measured using a CytoFluor 2350 fluorescence measurement system (Millipore, Bedford, MA). Mixtures of apo-NCS and ethidium bromide were prepared in specifically designed 96-well cytoplates (Millipore, Bedford, MA), and the fluorescence intensity for 5 μM ethidium bromide was monitored (λ_{ex} = 485 nm, λ_{em} = 590 nm) as a function of apo-NCS concentration.

(c) NMR Measurements. All NMR experiments were performed on a Bruker AM 500 spectrometer at 40 °C. Quadrature detection was used in both dimensions with the carrier frequency placed on the H_2O resonance for all experiments. Phase-sensitive DQF- and TQF-COSY (Piantini et al., 1982; Shaka et al., 1983), phase-sensitive RELAY (Eich et al., 1982; Bax et al., 1985), TOCSY (Bax et al., 1985), and clean TOCSY (Griesinger et al., 1988) were acquired in the TPPI mode with standard phase cycling schemes. The H_2O resonance was presaturated by selective irradiation for 1.5–2 s.

RELAY spectroscopy was performed with mixing times of 30 ms (90% H_2O) and 25 and 30 ms (99.8% D_2O). These mixing times were chosen to optimize the coherence transfer between the amide protons to the β protons of residues Ala, Phe, Val, Leu, etc. (Bax et al., 1985).

TOCSY spectroscopy was performed on samples of the ethidium bromide–NCS complex dissolved in both H_2O and D_2O. Experiments were carried out at a variety of mixing times ranging from 40 to 80 ms in order to optimize coherence transfer between spins of interest (Remerowski et al., 1989).

Several NOESY spectra were recorded at mixing times ranging from 100 to 200 ms, randomly varied by 10% (Anil Kumar et al., 1980). The spectral width was 8000 Hz (16 ppm). The data were collected with 1024 complex points in the t_2 dimension and 600 complex free induction decays (FIDs) in the t_1 dimension, and 64 transients were collected for each FID.

All data sets were transferred to a SGI Iris 4D/30 computer and processed with the program FELIX provided by Dr. Dennis Hare (Hare Research Inc., Woodinville, WA). The FIDs

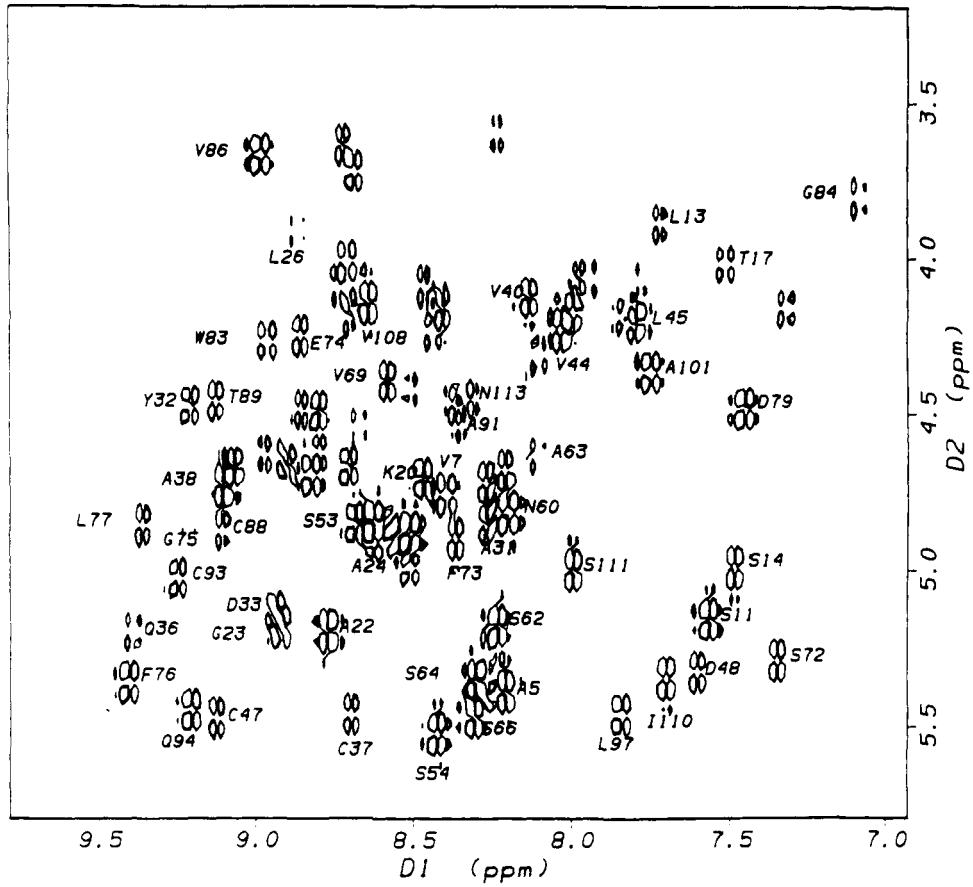

FIGURE 2: DQF-COSY fingerprint region of the aponeocarzinostatin–ethidium bromide complex in acetate buffer (90% H_2O/10% D_2O, pH 5.0) at 40 °C showing amino acid assignments.

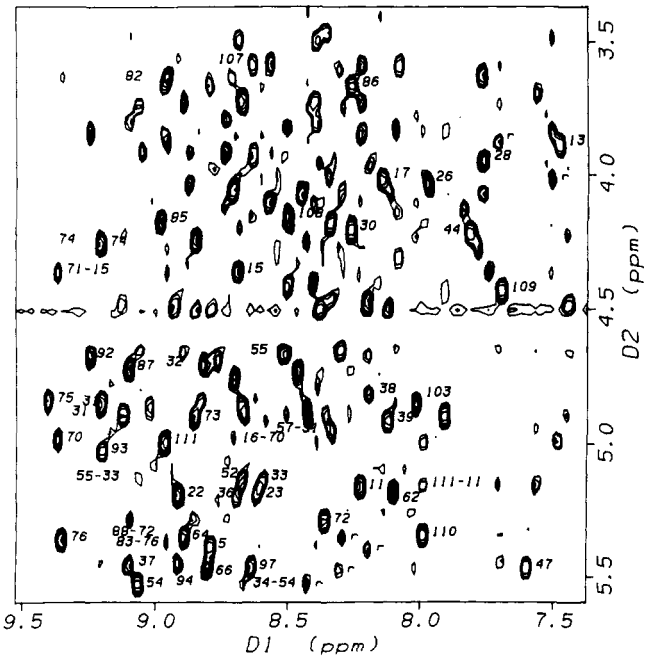

FIGURE 3: Two-dimensional NOESY spectrum of the apo-NCS–ethidium bromide complex in acetate buffer (90% H_2O/10% D_2O, pH 5.0) at 40 °C. The labeled cross peaks indicate $d_{\alpha N}$ connectivities. The labeling scheme is as follows: (1) cross peaks labeled with a single number are $d_{\alpha N}(i,i+1)$ NOEs connecting residue i to residue $i+1$; (2) cross peaks labeled with two numbers (i–j) are $d_{\alpha N}(i,j)$ long-range NOEs; (3) cross peaks labeled r are $d_{\alpha N}(i,i)$ intraresidue NOEs which have corresponding COSY cross peaks.

were apodized in both dimensions using skewed sine-bell functions, with a skew factor of 0.6–0.9 and a phase shift of 10–45. The first t_1 experiment was multiplied by 0.5 to suppress t_1 ridges in the spectra (Otting et al., 1985).

RESULTS

(a) Characterization of the 1:1 Complex between Aponeocarzinostatin and Ethidium Bromide. That the ethidium bromide binds to NCS was immediately evident from the one-dimensional ^1H NMR spectrum of the 1:1 complex in acetate buffer composed of 99.98% D_2O at pH 5.0. In particular, the methyl proton resonances of the apoprotein at –0.24 and –0.14 ppm in the high-field end of the spectrum were well resolved even in the one-dimensional NMR spectrum and were strongly perturbed upon binding to ethidium bromide. These methyl resonances, which were shifted from –0.24 and –0.14 ppm in apo-NCS to –0.78 and –0.87 ppm in the apo-NCS–ethidium bromide complex, were later assigned to Leu-45, which is known from NMR (Tanaka et al., 1993) and X-ray studies (Kim et al., 1993) to interact with the NCS chromophore. Strong perturbations of the proton resonances of a number of other protein residues were observed during the course of sequential assignment. These include Gln-36, Cys-37, Trp-39, Cys-47, Phe-52, Ser-98, and Gly-94. Another indication of drug binding was the large shifts of all the aromatic protons of ethidium bromide which were subsequently assigned using DQF-COSY, TOCSY, and NOESY.

(b) ^1H NMR Assignments for Aponeocarzinostatin in the 1:1 Complex. With a molecular weight of 11 100, NCS is a relatively large protein to be assigned by homonuclear 2D NMR. The protein has so far not been cloned, thus making isotopically labeled material unavailable at the present time. The apoprotein has been sequence-specifically assigned by a number of NMR groups using homonuclear 2D NMR (Remerowski et al., 1990; Adjadj et al., 1990) and homonuclear 3D NMR methods (Gao et al., 1991). However, the spectral changes observed upon complex formation were so extensive that the assignment process had to be repeated for the protein

Table 1: ^{1}H NMR Resonance Assignments[a] of the Aponeocarzinostatin–Ethidium Bromide Complex at 40 °C and pH 5.0

residue	NH	CαH	CβH	CγH	CδH	others
Ala-1						
Ala-2		4.640	1.330			
Pro-3		4.940	1.470, 2.0109	1.930, 1.880		
Thr-4	8.850	4.530	3.990	1.070		
Ala-5	8.200	5.420	1.080			
Thr-6	8.810	4.520	3.980	1.070		
Val-7	8.400	4.750	1.620	0.680, 0.570		
Thr-8	8.710	4.680	4.060	1.150		
Pro-9		4.990	2.540, 2.230	1.980, 1.740		
Ser-10	8.340	4.530	2.520			
Ser-11	7.560	5.190	3.710			
Gly-12	8.240	3.610	3.720			
Leu-13	7.720	3.930	0.580	1.030	0.380, 0.130	
Ser-14	7.480	5.020	3.730			
Asp-15		4.370				
Gly-16	8.700	4.220	3.530			
Thr-17	7.520	4.030	3.890	1.150		
Val-18	8.150		1.890	0.990, 0.810		
Val-19	9.120	4.660	1.980	0.790, 0.740		
Lys-20	8.470	4.700	1.750			
Val-21	8.900	4.660	1.590			
Ala-22	8.790	5.230	1.230			
Gly-23	8.930	5.210	3.080			
Ala-24	8.650	4.710	1.200			
Gly-25	8.700	3.740				
Leu-26	8.710	4.030	1.050	1.150	0.045, –0.060	
Gln-27	7.980	4.180				
Ala-28		3.980	1.300			
Gly-29	7.780	4.090	3.660			
Thr-30	7.810	4.210	4.290	0.870		
Ala-31	8.260	4.890	1.210			
Tyr-32	9.210	4.480	2.420			
Asp-33	8.930	5.120	2.250			
Val-34	8.620	4.540	1.770	0.680, 0.820		
Gly-35		4.560	3.180			
Gln-36	9.390	5.200	1.920, 2.350	1.700, 2.040		
Cys-37	8.700	5.500	2.530, 2.340			
Ala-38	9.130	4.800	1.170			
Trp-39	7.450	4.920	3.060			N1H 9.88; C2H 7.18; C4H 7.33; C5H 6.70; C6H 7.05; C7H 7.46
Val-40	8.130	4.140	1.380	0.013, –0.627		
Asp-41						
Thr-42	8.940	4.070	3.910			
Gly-43	8.770	3.810	4.120			
Val-44	8.040	4.240	1.640	0.800, 0.570		
Leu-45	7.350	4.200	0.977, 1.490	0.370	–0.780, –0.870	
Ala-46	8.510	4.910	0.830			
Cys-47	9.130	5.500	3.150, 2.870			
Asp-48	7.620	5.320	2.250			
Pro-49						
Ala-50	6.840	4.040	1.470			
Asn-51	6.320	5.060	2.220, 3.200			
Ph2-52	7.070	5.140	3.160, 2.880			C2, C6H, 6.50; C3, C5H 6.66; C4H 6.66
Ser-53	8.670	4.940	3.690			
Ser-54	8.420	5.570	3.770			
Val-55	9.060	4.660	1.990	0.670, 1.020		
Thr-56	8.500	4.910	3.850	1.000		
Ala-57	8.450	4.260	1.370			
Asp-58						
Ala-59		4.090	1.380			
Asn-60	8.220	4.800	2.770			
Gly-61	8.460	3.150	4.120			
Ser-62	8.220	5.210	3.870			
Ala-63	8.120	4.660	0.940			
Ser-64	8.290	5.350	3.760			
Thr-65	8.890	4.700	4.080	0.860		
Ser-66	8.300	5.500	3.650			
Leu-67	8.810	4.620	1.400	1.380	0.540, 0.930	
Thr-68		4.610	3.940	0.940		
Val-69	8.580	4.390				
Arg-70	8.750	4.98	1.610			
Arg-71	9.370	2.040	1.510			
Ser-72	7.290	5.320	3.500			
Phe-73	8.380	4.90				
Glu-74	8.850	4.270	2.050			
Gly-75	9.210	4.890	3.330			
Phe-76	9.400	5.350	2.690, 3.040			
Leu-77	9.350	4.850	2.040	1.750	0.740, 1.010	
Phe-78	9.130					

Table I (Continued)

residue	NH	CαH	CβH	CγH	CδH	others
Asp-79	7.620	4.410				
Gly-80	8.200	4.330	3.630			
Thr-81	8.020	4.060				
Arg-82	8.710	3.640				
Trp-83	8.980	4.290	2.700			N1H 10.23; C2H 6.91; C4H 7.07; C5H 6.85; C6H 7.14; C7H 7.39
Gly-84	7.120	3.500	3.830			
Thr-85	8.400	4.220	3.720	0.880		
Val-86	9.000	3.680	0.120	0.410		
Asn-87	8.270	4.720	2.930			
Cys-88	9.110	4.880	2.710			
Thr-89	9.120	4.460	4.250	1.170		
Thr-90	7.470	4.490	4.240	1.130		
Ala-91	8.360	4.490	1.170			
Ala-92	8.200	4.710	1.490			
Cys-93	9.280	5.030				
Gln-94	9.210	5.500	1.610, 2.050	1.850, 1.900		
Val-95	8.850	4.700	1.610			
Gly-96		4.280	3.720			
Leu-97	7.820	5.450	1.020, 1.580	1.290	0.280, 0.380	
Ser-98	8.630	5.180	3.180, 3.370			
Asp-99	8.930					
Ala-100	8.450	4.080	1.370			
Ala-101	7.800	4.400	1.370			
Gly-102	8.100	3.960	3.610			
Asn-103	8.650	4.840	3.000			
Gly-104	8.010	4.700	3.890			
Pro-105						
Glu-106						
Gly-107	8.700	3.340	4.160			
Val-108	8.660	4.160	1.830	0.980, 0.820		
Ala-109	8.520	4.460	1.490			
Ile-110	7.700	5.340	1.520	1.540 (CγH3 0.760)		
Ser-111	8.000	5.070	3.870			
Phe-112	8.980	4.630	2.520			
Asn-113	8.320	4.450	2.620			

[a] Chemical shifts in ppm (±0.02) have been referenced to the H_2O resonance at 4.60 ppm at 313 K in 10 mM acetate buffer and 0.1 mM EDTA.

in the complex virtually from the beginning. Assignment of the protein in the complex was more difficult due to severe spectral overlap of the protein resonances caused by both line broadening and the strong chemical shift perturbation upon binding to ethidium bromide which degraded resolution in a number of areas of the protein spectrum. Nevertheless, apo-NCS in the complex was successfully assigned following the two-step procedure developed by Wüthrich (1986), i.e., identification of the spin system followed by sequence-specific assignment of these spin systems to specific amino acid residues in the protein.

Different spin systems were identified using various coherence transfer experiments. The CαH–CβH3 cross peaks of Ala and CβH–CγH3 cross peaks of Thr residues were identified using D_2O DQF–COSY and RELAY. The side chains of Leu and Val were identified using D_2O TOCSY. We identified CαH–CβH cross peaks of 10 out of 11 serines using D_2O TQF-COSY. The CαH–Cα′H cross peaks of Gly were identified by the use of both DQF- and TQF-COSY experiments recorded in 99.98% D_2O. The DQF-COSY spectrum in H_2O was used to connect an individual amide proton to its Cα proton(s). The H_2O RELAYED-COSY helped to connect the amide protons to its Cβ proton(s). When the mixing time in the RELAY experiment was optimized, the coherence transfer from the amide to the β protons of various residues like Ala, Val, Leu, and Phe was achieved (Bax et al., 1985). The H_2O TOCSY spectrum allowed further extension of these connectivities to side-chain protons.

(c) Sequential Assignment. After the identification of the few unique amino acid spin systems using DQF-COSY, TQF-COSY, RELAY, and TOCSY, the next step in the sequential assignment process was to assign each spin system to specific residues by combining the information of the COSY and NOESY spectra obtained in H_2O.

Except for the terminal residues Ala-1 and Ala-2 and a few other residues such as Asp-15, Gly-35, Ala-28, Asp-41, Asp-58, and Ala-59 whose amide–CαH cross peaks were not observed, most other fingerprint cross peaks appeared in either DQF-COSY, RELAY, or TOCSY spectra, thus facilitating the sequential assignment. Some fingerprint cross peaks like Phe-52 and Gly-84 appeared only in RELAY or TOCSY spectra. Figures 2 and 3 show the fingerprint section of DQF-COSY and NOESY spectra, respectively, each recorded at 40 °C. As in apo-NCS, sequential connectivities were accomplished primarily through $d_{\alpha N}$ connectivities. The long stretches of $d_{\alpha N}$ connectivity were broken at a few places, primarily at the four proline residues at Pro-3, Pro-9, Pro-49, and Pro-105. The first break in the $d_{\alpha N}$ connectivity pattern occurs at Pro-9. The long stretch from Pro-9 to Gly-16 has a very irregular connectivity pattern, which indicates that this stretch does not have any regular secondary structure and is a wide "bubble" or loop, which was present in the free protein also (Remerowski et al., 1990). Besides the breaks at proline residues, there were a few other short breaks of two to three residues in the $d_{\alpha N}$ connectivity pattern. These breaks are at places where a gradual chain reversal in the β-strand occurred, causing a slight bend or twist at that point. The first such break due to chain reversal occurs at Gly-29. There is virtually no break between Thr-30 and Val-40. The connectivity sequence between Val-40 and Val-44 is interrupted at Gly-43 due to a turn in the β-strand which is manifested by a single d_{NN} NOE connecting Gly-43 to Val-44. Between Val-44 and Phe-52 there is a break due to a proline residue at Pro-49 and also a turn between Asn-51 and Phe-52, which is indicated

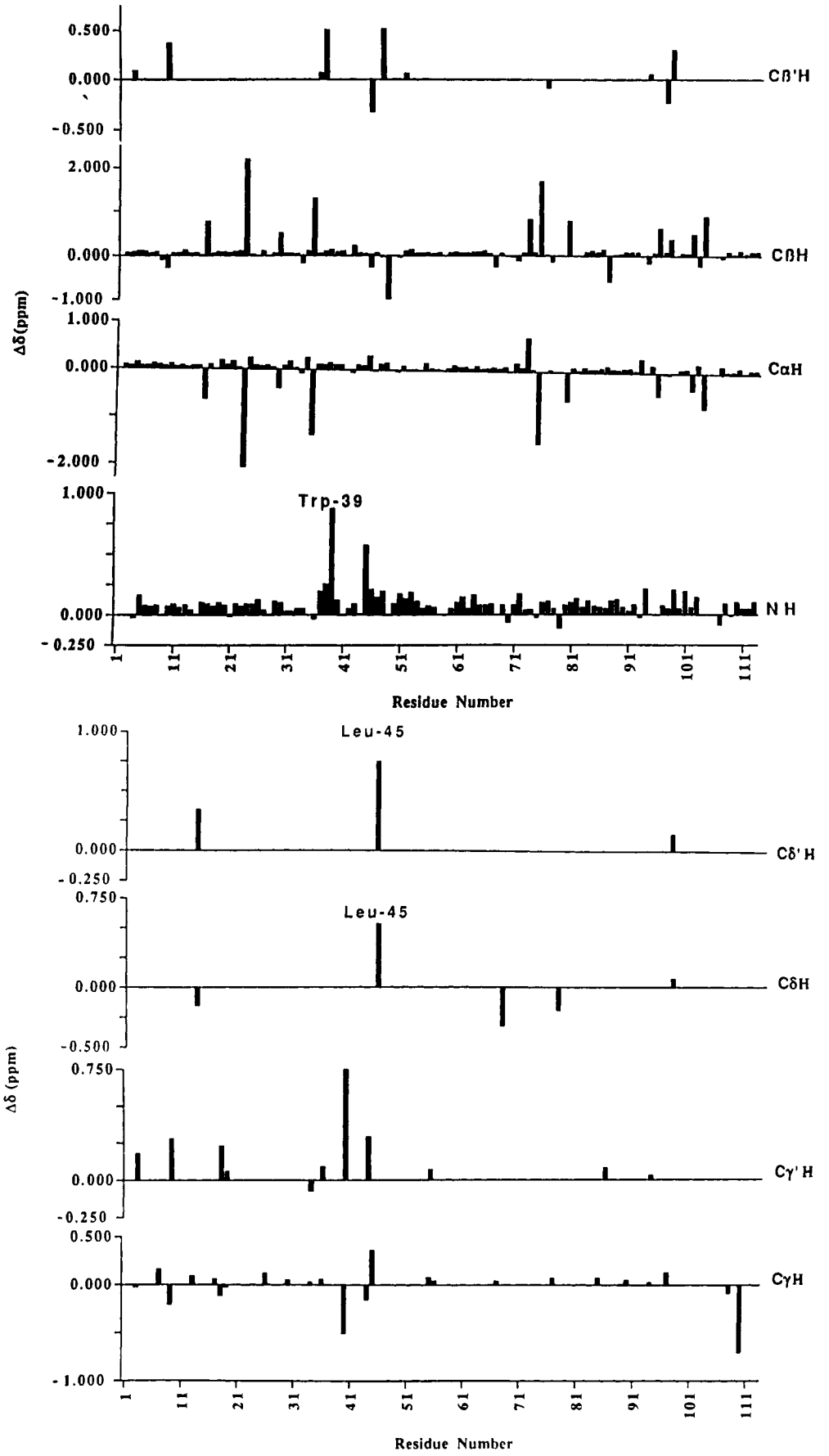

FIGURE 4: Schematic diagram showing the changes in the chemical shifts of aponeocarzinostatin protons induced upon binding to ethidium bromide. Positive values indicate that the resonances in the complex are at higher field than in the free protein.

by the strong d_{NN} NOE between Asn-51 and Phe-52. The $d_{\alpha N}$ connectivity continues unbroken from Phe-52 to Ala-57 and from Ser-62 to Arg-70. The break at Asp-58 and Ala-59 is due to chain reversal of the β-strand. Residues Ser-72 to Asn-87 form a loop consisting of two antiparallel β-strands with a chain reversal occurring in the region Phe-78 to Thr-

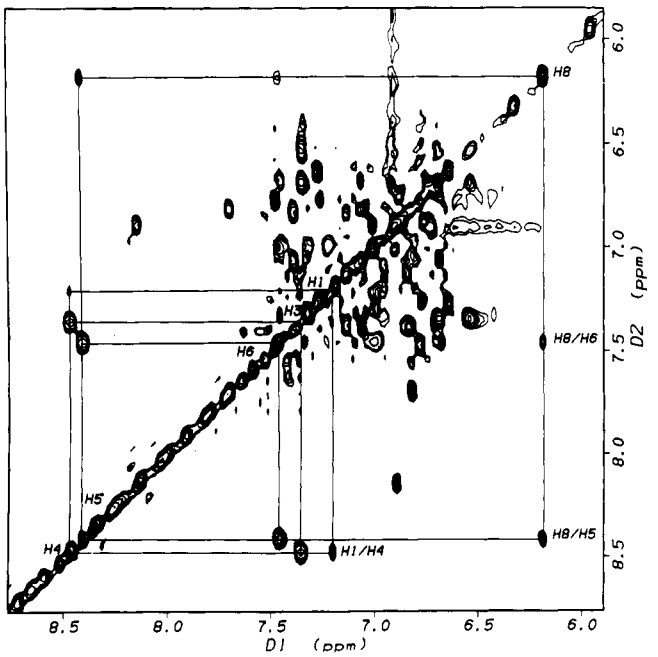

FIGURE 5: Aromatic region of the D_2O TOCSY (99.98% D_2O, pH 5.0, 40 °C) spectrum of the aponeocarzinostatin–ethidium bromide complex showing both ortho and meta coupling in the phenanthridine ring system of ethidium bromide.

81. The last two breaks in the $d_{\alpha N}$ connectivity pattern due to chain reversal occur at Thr-90 and Ala-100. However, the sequential assignment was continued by finding the d_{NN} or $d_{\beta N}$ connectivities at those break points. Chemical shift assignments for NCS in the complex with ethidium bromide are given in Table 1.

(d) Change in Chemical Shifts for Protein Protons in the Complex. Large changes in ^1H chemical shifts were observed for many residue protons of the protein in the drug–protein complex. Most apparent of these were the methyl proton resonance lines of Leu-45, which are resolved even in the 1D spectrum. Large upfield shifts were also readily observed for the H2′, H6′ and H3′, H4′, H5′ ring protons of Phe-52. The H2′, H6′ and H3′, H4′, H5′ ring protons of Phe-52, which in apo-NCS are overlapped with the H2′, H6′ and H3′, H4′, H5′ protons of the four other phenylalanines and the single tyrosine in the apoprotein, had undergone large upfield shifts and as a result were resolved from the other phenylalanine resonances in the complex. These Phe-52 ring protons were identified through NOE connectivities to their own CHβ and CHβ′ protons. Chemical shift changes were also observed for the amide and the Cα protons of Gln-36, Cys-37, Ala-38, Trp-39, Leu-45, Cys-47, Asp-48, Cys-93, Gln-94, and Leu-97. Figure 4 summarizes the changes in the chemical shifts of protein protons induced by drug binding.

(e) Conformation of Aponeocarzinostatin in the 1:1 Complex. Both the crystal structure (Sieker, 1981) and the NMR (Adjadj et al., 1990, 1992; Remerowski et al., 1990; Gao et al., 1991) work done on apo-NCS indicate that a major part of the protein consists of a seven-strand antiparallel β-barrel formed by a three-strand β-sheet and a four-strand β-sheet arranged in a Greek key. The rest of the protein is composed of two loops which lie at the base of the barrel orienting somewhat perpendicular to it, thus forming a distinct U-shaped cleft between the four-strand face of the barrel and one of the loops of the molecule.

On the basis of our data on the interstrand long-range backbone NOEs and slowly exchanging amide protons, we see three antiparallel β-sheeted structural domains of the protein in the complex: the external three-strand β-sheet (Thr-4–Thr-8; Thr-17–Ala-24; Ser-62–Val-69), the internal four-strand β-sheet (Thr-30–Val-40; Phe-52–Ala-57; Cys-93–Asp-99; Gly-107–Ile-110), and the small two-strand β-sheet (Ser-72–Phe-76; Arg-82–Asn-87).

The external three-strand β-sheet has strand 1 (Thr-4–Thr-8) running antiparallel to residues (Lys-20–Ala-24) of the middle strand. The middle strand (Thr-17–Ala-24) forms an antiparallel β-sheet with strand 3 (Ser-62–Val-69).

The internal four-strand β-sheet has strand 4 (Thr-30–Val-40) running antiparallel to strand 5 (Phe-52–Ala-57) on one side and to the strand 6 (Cys-93–Asp-99) on the other side. Strand 7 (Gly-107–Ile-110) runs antiparallel to the strand 6 (Cys-93–Asp-99). Residues Cys-37–Cys-47 of this four-strand β-sheet form an external small loop.

The small two-strand β-sheet has one strand (Ser-72–Phe-76) which runs antiparallel to the second strand (Arg-82–Asn-87) forming a loop.

The pattern of intermolecular NOE connectivities suggests that the secondary structure of the protein in the complex with ethidium bromide is very similar to that of the free protein in solution, thus indicating that the secondary structure of the protein is conserved in the complex.

(f) Assignment of Ethidium Bromide in the Complex. The ethidium bromide proton resonances in the complex were assigned using DQF-COSY, TOCSY, and NOESY experiments. Of the six phenanthridine ring protons (see Figure 1b for numbering), H3 is strongly coupled to H4 (ortho coupling, 9–10 Hz) and is weakly coupled to H1 (meta coupling, 1–2 Hz). Similarly, H5 is strongly coupled to H6 (ortho coupling) and is meta coupled to H8.

Both of the strongly coupled ortho pairs (H3–H4 and H5–H6) were identified from the DQF-COSY spectrum. However, the meta coupling was not observed in the DQF-COSY spectrum, thus making it impossible to differentiate the H1, H3, and H6 spin system from the H5, H6, and H8 spin system. This ambiguity was solved using a TOCSY experiment. The appearance of meta- as well as para-coupled peaks in the TOCSY spectrum (Figure 5) helped to identify these two systems and enabled the assignment of H1 and H8. The H8 resonance was obviously the most upfield of all these six protons as it was in the shielding region of the neighboring phenyl ring and therefore experienced a magnetic anisotropy effect from the ring current of the phenyl ring. This through-bond assignment was confirmed in the NOESY spectrum (Figure 6) where a strong NOE was observed between H4 and H5 along with other weak NOEs from H8 to H6 and H5.

The phenyl ring proton cross peaks were identified in the DQF-COSY on the basis of the NOE cross peaks to H8. The H2′ and H6′ protons of the phenyl ring were overlapped and showed strong NOEs to H8. The H3′, H4′, and H5′ protons of the phenyl ring were also overlapped and showed weak NOEs to H8. The alkyl side chain was assigned by identifying the NOE to H1 and to the H2′, H6′ of the phenyl ring. The assignment of the proton resonances of both free and bound ethidium bromide is given in Table 2.

(g) Intermolecular Contacts between Ethidium Bromide and NCS. Once sequence-specific resonance assignments for both components of the complex were achieved, the next step was to identify contacts between apo-NCS and ethidium bromide, which are directly manifested as intermolecular NOEs. We have detected a number of intermolecular NOEs between the protein protons and ethidium bromide protons in the NOESY spectrum of the complex. The H4 proton on the phenanthridine ring of ethidium bromide shows a strong NOE to the methyl protons (δ) of Leu-45 at –0.87 ppm and a weak NOE to the methyl protons of Leu-45 at –0.78 ppm. It also

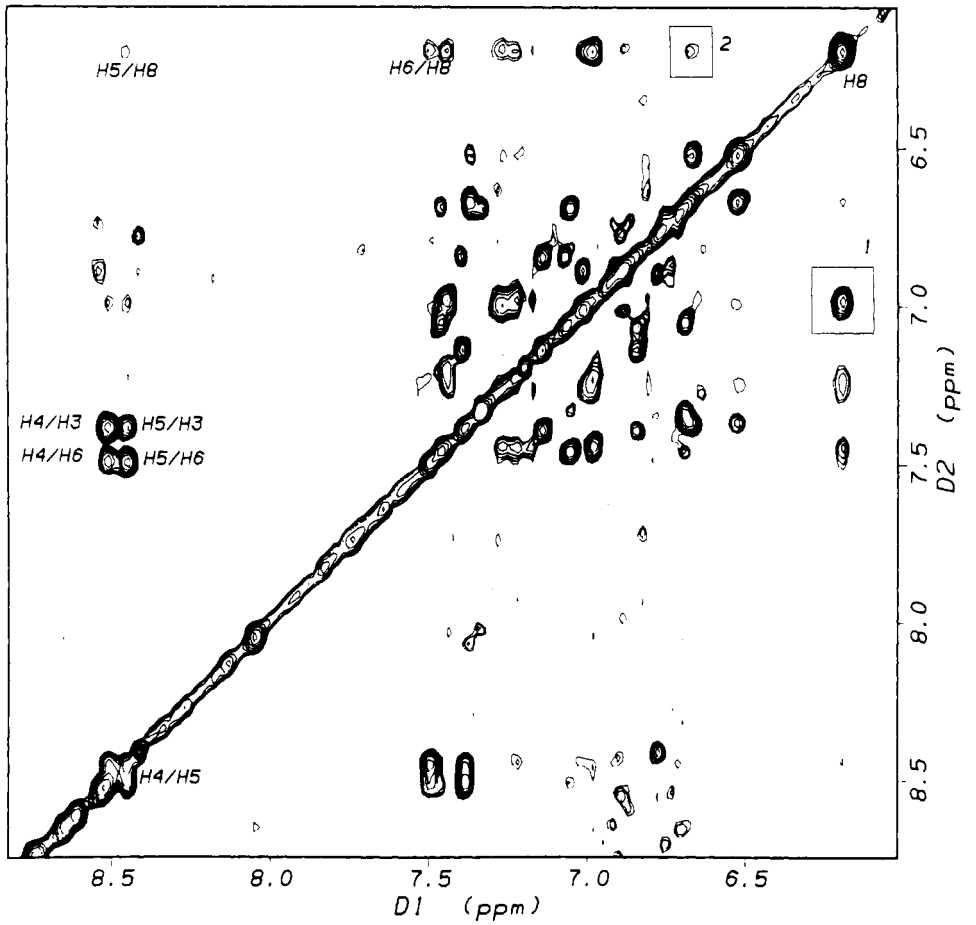

FIGURE 6: Aromatic region of the D_2O NOESY (99.98% D_2O, pH 5.0, 40 °C) spectrum of the aponeocarzinostatin–ethidium bromide complex showing intramolecular NOEs for the ethidium bromide protons. The cross peaks within the box are (1) the intramolecular NOE between H8 and H2′, H6′ of the phenyl ring and (2) the intermolecular NOE between H8 and C3′,4′,5′H of Phe-52.

Table 2: Proton Chemical Shifts in ppm of Free Ethidium Bromide vs Ethidium Bromide Bound to the Aponeocarzinostatin at pH 5.0, 313 K

	free	complex		free	complex
phenanthridine ring system			alkyl side chain		
			CH_2	4.38	4.41
H1	7.16	7.21	CH_3	1.24	1.04
H3	7.13	7.38	phenyl ring		
H4	7.95	8.50	H(2′,6′)	7.16	6.98
H5	7.83	8.48	H(3′,5′,4′)	7.70	7.24
H6	7.22	7.49			
H8	6.26	6.18			

shows an NOE to C6H of the indole ring of Trp-39. Similarly, H6 on the phenanthridine ring of ethidium bromide shows a strong NOE to Gln-94's β-methylene protons and also to the (δ) methyl protons (–0.78 ppm) of Leu-45. The H8 and the phenyl ring protons of ethidium bromide show NOEs to Cβ′H of Cys-47, the methyl protons of Leu-45 (–0.78 ppm), and the C3′,4′,5′H of Phe-52 ring protons of the protein. The phenyl ring of ethidium bromide shows NOEs to the C3′,4′,5′- of Phe-52 (Figure 6). Some of these NOEs are shown in a NOESY spectrum of the complex acquired at 40 °C with a 150-ms mixing time (Figure 7). A complete list of all unambiguously assigned intermolecular NOEs is given in Table 3.

DISCUSSION

(a) Comparison of Protein–Drug Interactions in the Apo-NCS–Ethidium Bromide Complex with the Protein–Drug Interactions Observed in the X-ray and NMR-Derived Structures of Holo-NCS. In the crystal structure of holo-NCS (Kim et al., 1993) the two π-faces of the enediyne ring of NCS-Chr are sandwiched between the aromatic rings of Phe-78 and Phe-72 on one side and the disulfide bond of Cys-37–Cys-47 on the other side. The naphthoate group resides at the bottom of the cleft and forms hydrogen bonds to the carbonyl oxygen and Oγ of Ser-98 and the methoxy oxygen and the amide proton of Gly-35. Numerous van der Waals contacts occur between the naphthoate and enediyne moieties of NCS-Chr and apolar residues of the protein including Gly-35, Leu-45, Pro-49, Leu-77, Gly-80, Val-95, Gly-96, Ala-101, and Gly-102 and the aromatic residues Trp-39, Phe-52, Phe-76, and Phe-78. The only polar residues near the chromophore are Gln-94 and Ser-98. The orientation of the chromophore in the cleft of NCS obtained by X-ray diffraction generally agrees with the orientation obtained by Tanaka et al. (1993) using NMR.

Comparison of the drug–protein NOEs observed for the ethidium–NCS complex (Table 3) and intermolecular NOEs observed between the chromophore and the protein in holo-NCS (Tanaka et al., 1991, 1993) indicates that ethidium forms a 1:1 complex with apo-NCS and binds in the same cleft within which the chromophore resides in holo-NCS. Specifically, the protons of the phenanthridine ring system of ethidium show NOEs to most of the amino acid residues which are reported to have NOEs to the naphthoate or the enediyne moieties of the NCS chromophore (Tanaka et al., 1991, 1993). For example, H7 of Trp-39 shows an NOE to H3″ of the naphthoate ring of NCS-Chr whereas H6 of Trp-39 shows an NOE to H4 of the phenanthridine ring of ethidium. CβH of Ser-98 shows NOEs to the H8″ and 7″ methoxy protons of

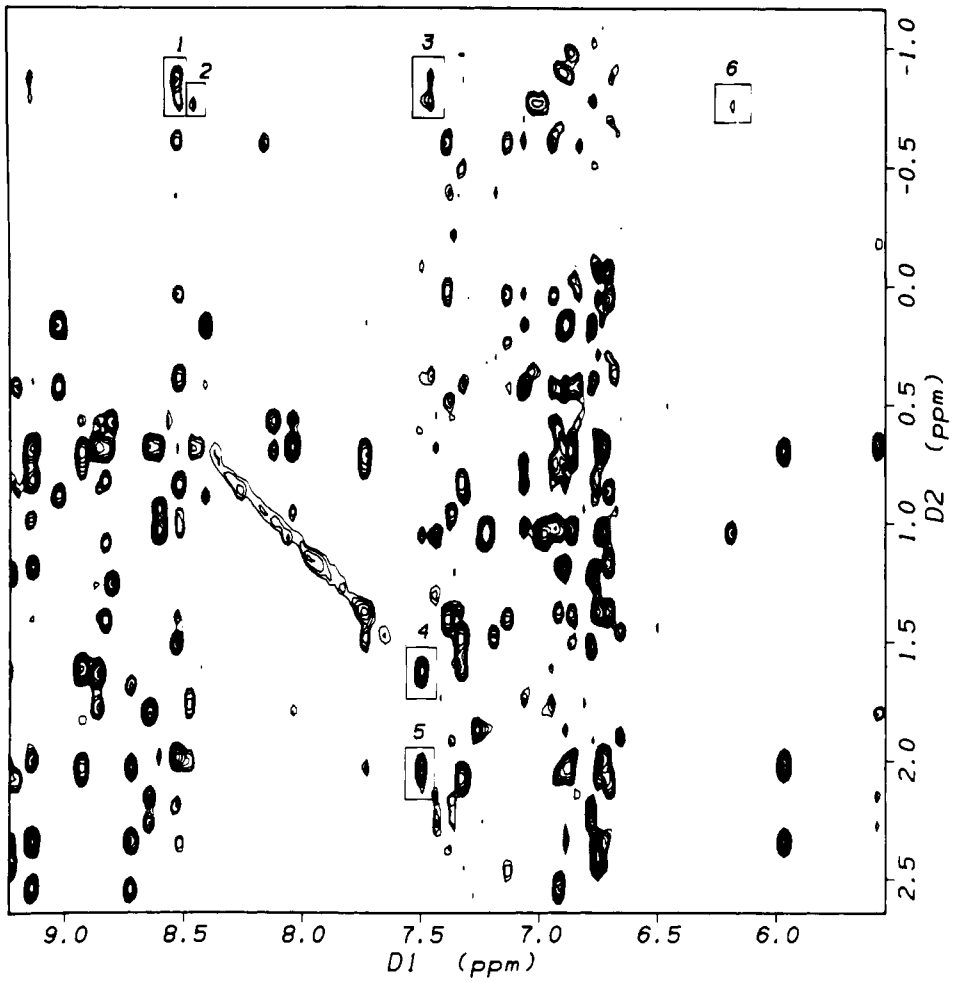

FIGURE 7: The region of the 500-MHz D_2O NOESY (t_m = 150 ms) spectrum of the aponeocarzinostatin–ethidium bromide complex containing some of the intermolecular NOEs between the protein and the drug. The intermolecular NOEs that are identified in this contour plot are as follows: (1) Leu-45 CH_3(d)/H4; (2) Leu-45 CH_3(d)/H5; (3) Leu-45 CH_3(d)/H3; (4) Gln-94 βH/H6; (5) Gln-94 β′H/H6; (6) Leu-45 CH_3(d)/H8.

Table 3: Intermolecular NOEs Observed between Protons of Aponeocazinostatin and Ethidium Bromide in the 1:1 Complex (pH 5.0, 313 K)

	intramolecular NOEs	intermolecular NOEs
phenanthridine ring system		
H1 (7.22)	CH_2, CH_3	
H3 (7.38)	H4, H5	Ser-98 CβH, Leu-45 CδH3 (–0.73)
H4 (8.51)	H3, H5, H6	Leu-45 CδH3 (–0.83), Trp-39 C6H
H5 (8.48)	H4, H6, H3, H8	Leu-45 CδH3 (–0.73), Gln-94 CβH
H6 (7.49)	H5, H4, H8	Gln-94 CβH, Gln-94 Cβ′H, Leu-45 CδH3 (–0.73)
H8 (6.18)	H2′, H6′, H3′, H5′	Cys-47 Cβ′H, Leu-45 CδH3 (–0.73), Phe-52 C3′,4′,5′H
alkyl side chain		
CH_2 (4.41)	H1, CH_3, H2′,6′, H3′, H5′	
CH_3 (1.04)	CH_2, H1, H2′,6′, H3′, H5′	
phenyl ring		
H2′,6′ (6.98)	H8, H3′,5′, H4′, CH_2, CH_3	Phe-52 C3′,4′,5′H
H3′,5′,4′ (7.44)	H8,H2′,6′, CH_2, CH_3	Phe-52 C3′,4′,5′H

the naphthoate moiety in holo-NCS and shows an NOE to H3 of the phenanthridine system in the ethidium–NCS complex. In holo-NCS the H3, H4, and H5 protons of Phe-52 have NOEs to the 7″ methoxy protons of the naphthoate ring whereas in the ethidium–NCS complex these residue protons show NOEs to H8 of the phenanthridine ring and the protons of the phenyl ring of ethidium as well. The CδH protons of Leu-45 show NOEs to H8 and H10 of the enediyne ring of the chromophore in holo-NCS whereas these same protons have NOEs to H3, H4, H5, and H8 of the phenanthridine in the ethidium–NCS complex. Evidently the large upfield shifts of the CδH methyl protons of Leu-45 upon complexation of apo-NCS to NCS-Chr or ethidium are due to the ring currents from the π systems of the enediyne of the chromophore in holo-NCS and the phenanthridine ring of ethidium.

An additional intermolecular NOE was detected between the methylene protons of ethidium and aromatic protons of the protein at 6.97 ppm. Unfortunately, this region of the NOESY spectrum was heavily crowded by the aromatic protons of Phe-73, Phe-76, Phe-78, Phe-112, and Tyr-32. Reference to Figure 4, however, shows that the residue protons of Phe-78 are strongly perturbed upon binding to ethidium so it is likely that this NOE is to Phe-78. If this tentative assignment is accepted, then ethidium is binding in the same vicinity of the cleft in which the enediyne and naphthoate

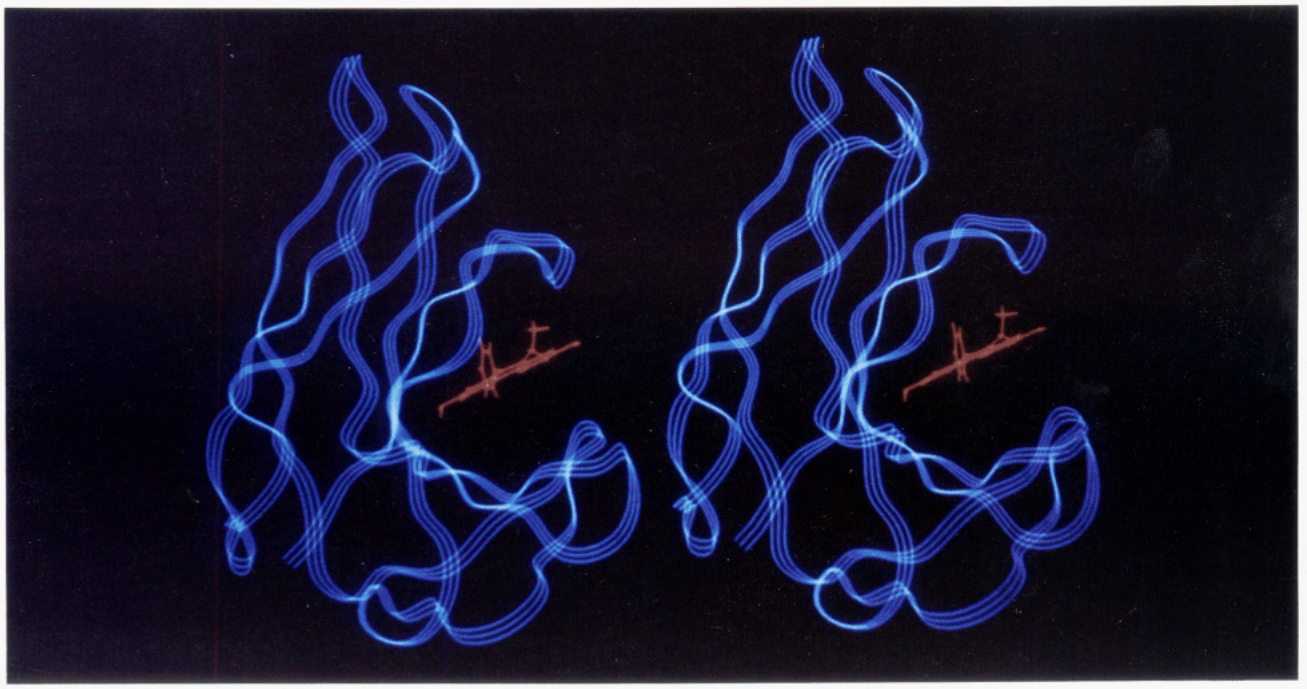

FIGURE 8: Stereoview of the ribbon diagram of apo-NCS with the ethidium molecule (shown in red) docked to the binding pocket, taking into account all intermolecular NOEs observed.

moieties reside and are sandwiched by Phe-52, Phe-78, and the Cys-37–Cys-47 disulfide bond.

Although many amino acid residues of NCS show NOEs to both the chromophore and ethidium, there are a number of differences. In holo-NCS a number of naphthoate protons show NOEs to the NH and CαH of Val-95 and the NH of Gly-96, whereas no NOEs between these residue protons and protons on ethidium are detected. Finally, the only residue which appears to show an NOE to ethidium but has no NOEs to the chromophore nor is reported have contacts to the chromophore in the crystal structure of holo-NCS is Asn-103, whose NH proton has an NOE to the methyl protons of ethidium.

To aid in the visualization of the binding of ethidium to apo-NCS and to provide a rough comparison to the binding of the chromophore in holo-NCS as reported in the X-ray study by Kim et al. (1993) and the NMR study of Tanaka et al. (1993), the structure of ethidium docked to the 1.8-Å apo-NCS crystal structure (Sieker and Ramanadan, private communication) is shown in Figure 8. Model building was accomplished using FRODO version E3.2 (Jones, 1978) on an Evans and Sutherland PS390 color graphics system, where the docking was performed to conform with the intermolecular NOEs reported in Table 3.

(b) Comparison of the Dissociation Constant (K_d) for the Ethidium–NCS Complex versus the K_d for the Chromophore–NCS Complex. A Scatchard analysis of fluorescence quenching of the chromophore by apo-NCS indicates very tight binding, with a K_d on the order of 0.1 nM (Goldberg et al., 1981). Tanaka et al. (1993) have suggested that interactions between the protein and the naphthoate group of the chromophore, which inserts deep into the cleft, are essential for the specific and tight binding of the chromophore to apo-NCS. Figure 8 indicates that the phenanthridine ring of ethidium bromide also inserts into the same region of the cleft, and proton NOEs reported in Table 3 suggest that the phenanthridine ring interacts with essentially the same amino acid residues as the naphthoate and enediyne groups of the chromophore. However, fluorescence measurements on the ethidium bromide–apo-NCS complex yield a K_d of 8.57×10^{-7} M, indicating that binding between ethidium bromide and apo-NCS is much less tight than between the chromophore and apo-NCS.

The differences in the tightness of binding of ethidium bromide versus the chromophore to apo-NCS may derive from the numerous hydrogen-bonding and hydrophobic interactions that occur between amino acid residues of the protein and various functional groups on the chromophore which do not occur in the apo-NCS–ethidium complex. For example, the fact that D-galactosamine displaces the chromophore at the binding site but not D-galactose indicates that the amino group of the sugar moiety plays an important role in binding of the chromophore to the protein (Ishiguro et al., 1991). A molecular modeling study by Ishiguro et al. (1991) describes numerous hydrogen-bonding interactions between the chromophore and amino acid residues of the protein including a hydrogen bond between the hydroxyl group of the *N*-methylfucosamine moiety and Asp-99 and a hydrogen bond between the carbonate carbonyl group of the chromophore and Ser-98. The fact that β-naphthol displaces the chromophore but not α-naphthoic acid also suggests that the hydroxyl group of the naphthoate moiety plays an important role in chromophore binding. Accordingly, the molecular modeling study of Ishiguro et al. (1991) predicts a hydrogen bond between the phenolic group at C2″ on the chromophore and the carbonyl oxygen of Phe-76.

CONCLUSION

The total assignment of the apo-NCS–ethidium bromide complex based on coherence transfer experiments and nuclear Overhauser studies indicates that ethidium bromide binds to a single site within the chromophore binding cleft of NCS. The conclusion that the ethidium bromide binds to apo-NCS within the the chromophore binding cleft is based upon the observation of more than 20 intermolecular NOEs that were observed between protons on ethidium bromide and protons of amino acid residues which also display NOEs to the chromophore in holo-NCS (Tanaka et al., 1991) or which are observed to have van der Waals interactions to the chromophore in the crystal structure (Kim et al., 1993). One such

important interaction is the intermolecular NOE observed between the H4 proton on the phenanthridine ring system of the ethidium bromide to the Leu-45 δ-methyl proton of the protein and that of the H8 proton on the enediyne system of the chromophore to the Leu-45 δ-methyl proton of the protein. Other such important interactions which are common for both the drugs are those to protons on residues Trp-39, Ser-98, and Phe-52 of the protein (Tanaka et al., 1991). On the basis of the NOE data a preliminary picture of ethidium's binding to apo-NCS (Figure 8) places the phenanthridine ring in the vicinity of the residues of Phe-52, Phe-78, and Cys-47, where the crystal structure of Kim et al. (1993) places the enediyne ring of the chromophore.

ACKNOWLEDGMENT

We gratefully acknowledge the assistance of Prof. Ronald Stenkamp and Dr. Vivian Yee for their help with the computer graphics system, Prof. Rachel Klevit for helpful discussions, and Dr. M. Ramanadham for the coordinates of apo-NCS at 1.8 Å. We thank Kayaku Co. Ltd. of Tokyo, Japan, for providing us with holo-NCS.

REFERENCES

Adjadj, E., Mispelter, J., Quiniou, E., Dimicoli, J., Favaudon, V., & Lhoste, J. (1990) Proton NMR studies of apo-neocarzinostatin from *Streptomyces carzinostaticus*. Sequence specific assignment and secondary structure, *Eur. J. Biochem. 190*, 263–271.

Adjadj, E., Quiniou, E., Mispelter, J., Favaudon, V., & Lhoste, J. (1992) Three-dimensional solution structure of apo-neocarzinostatin from *Streptomyces carzinostaticus* determined by NMR spectroscopy, *Eur. J. Biochem. 203*, 505–511.

Anil Kumar, Ernst, R. R., & Wüthrich, K. (1980) A two-dimensional nuclear Overhauser enhancement (2D NOE) experiment for the elucidation of complete proton–proton cross-relaxation networks in biological macromolecules, *Biochem. Biophys. Res. Commun. 95*, 1–6.

Bax, A., & Davis, D. G. (1985) MLEV-17 based two-dimensional homonuclear magnetization transfer spectroscopy, *J. Magn. Reson. 65*, 355–360.

Bax, A., & Drobny, G. P. (1985) Optimization of two-dimensional homonuclear relayed coherence transfer NMR spectroscopy, *J. Magn. Reson. 61*, 306–320.

Dasgupta, D., & Goldberg, I. H. (1985) Mode of reversible binding of neocarzinostatin chromophore to DNA: Evidence for binding via the minor groove, *Biochemistry 24*, 6913–6920.

Dikinson, L., Chanttill, B. H., Inkley, G. W., & Thompson, M. J. (1953) The antiviral action of phenanthridinium compounds, *Br. J. Pharmacol. 8*, 139.

Edo, K., Mizugaki, M., Koide, Y., Seto, H., & Ishida, N. (1985) The structure of neocarzinostatin chromophore possessing a novel bicyclo[7.3.0]dodecadiyne system, *Tetrahedron Lett. 26*, 331–334.

Eich, G., Bodenhausen, G., & Ernst, R. R. (1982) Exploring nuclear spin systems by relayed magnetization transfer, *J. Am. Chem. Soc. 104*, 3731–3732.

Elliott, W. H. (1963) The effects of antimicrobial agents on deoxyribonucleic acid polymerase, *Biochem. J. 86*, 562–567.

Favaudon, V., Charnas, R. L., & Goldberg, I. H. (1985) Poly(deoxyadenylic–deoxythymidylic acid) damage by radiolytically activated neocarzinostatin, *Biochemistry 24*, 250–259.

Gao, X. (1992) Three-dimensional solution structure of apo-neocarzinostatin, *J. Mol. Biol. 225*, 125–135.

Gao, X., & Burkhart, W. (1991) Two- and three-dimensional proton NMR studies of apo-neocazinostatin, *Biochemistry 30*, 7730–7739.

Goldberg, I. L., Hatayama, T., Kappen, L. S., Napier, M. A., & Povirk, L. F. (1981) *Molecular Actions and Targets for Cancer Chemotherapeutic Agents*, Vol. 1, pp 163–191, Academic Press, New York.

Griesinger, C., Otting, G., Wüthrich, K., & Ernst, R. R. (1988) Clean-TOCSY for ^{1}H spin system identification in macromolecules, *J. Am. Chem. Soc. 110*, 7870–7872.

Henderson, J. F. (1963) Inhibition of purine metabolism in Ehrlich ascites carcinoma cells by phenanthridinium compounds related to ethidium bromide, *Cancer Res. 23*, 491–495.

Ishida, N., Miyazaki, K., Kumgai, K., & Rikimaru, M. (1965) Neocarzinostatin, an antitumor antibiotic of high molecular weight, *J. Antibiot. A18*, 68–76.

Ishiguro, M., Imago, S., & Hirama, M. (1991) Modeling Study of the structure of the macromolecular antitumor antibiotic neocarzinostatin. Origin of the stabilization of the chromophore, *J. Med. Chem. 34*, 2366–2373.

Jones, T. A. (1978) A graphics model building and refinement system for macromolecules, *J. Appl. Crystallogr. 11*, 268–272.

Kappen, L. S., & Goldberg, I. H. (1980) Stabilization of neocarzinostatin nonprotein chromophore activity by interaction with apoprotein and with HeLa cells, *Biochemistry 19*, 4786–4790.

Kappen, L. S., & Goldberg, I. H. (1989) Identification of 2-deoxyribonolactone at the site of neocarzinostatin-induced cystosine release in the sequence d(AGC), *Biochemistry 28*, 1027–1032.

Kappen, L. S., & Goldberg, I. H. (1993) Site-specific cleavage at a DNA bulge by neocarzinostatin chromophore via a novel mechanism, *Biochemistry 32*, 13138–13145.

Kappen, L. S., Goldberg, I. H., & Samy, T. S. A. (1979) Contrasts in the actions of protein antibiotics on deoxyribonucleic acid structure and function, *Biochemistry 18*, 5123–5127.

Kappen, L. S., Napier, M. A., Goldberg, I. H., & Samy, T. S. A. (1980) Requirement of reducing agents in deoxyribonucleic acid strand scission by the purified chromophore of auromomycin, *Biochemistry 19*, 4780–4785.

Kappen, L. S., Goldberg, I. H., & Liesch, J. M. (1982) Identification of thymidine-5′-aldehyde at DNA strand breaks induced by neocarzinostatin chromophore, *Proc. Natl. Acad. Sci. U.S.A. 79*, 744–748.

Khokholov, A. S., Reshetov, P. D., Chupova, L. A., Cherches, B. Z., Zhigis, L. H., & Stoyachenko, I. A. (1976) Chemical studies on Actinoxanthin, *J. Antibiot. 29*, 1026–1034.

Kim, K.-H., Kwon, B.-M., Meyers, A. G., & Reese, D. C. (1993) Crystal Structure of Neocarzinostatin, an antitumor protein–chromophore complex, *Science 262*, 1042–1046.

Kumada, Y., Miwa, T., Naoi, N., Watenabe, K., Naganawa, H., Takita, T., Umezawa, H., Nakamura, H., & Iitaka, Y. (1983) A degradation product of the chromophore of auromomycin, *J. Antibiot. 36*, 200–202.

Maeda, H., Aikawa, S., & Yamashita, A. (1975) Subcellular fate of protein antibiotic neocarzinostatin in culture of a lymphoid cell line from Burkitt's lymphoma, *Cancer Res. 35*, 554–559.

Meschwitz, S., Schultz, R. G., Ashley, G. W., & Goldberg, I. H. (1992) Selective abstraction of ^{2}H from C-1′ of the C residue in AGC·ICT by the radical center at C-2 of activated neocarzinostatin chromophore: structure of the drug/DNA complex responsible for bistranded lesion formation, *Biochemistry 31*, 9117–9121.

Montgomery, R., Shepherd, V. L., & Vandre, D. D. (1981) *Antitumor Compounds of Natural Origin: Chemistry and Biochemistry*, Vol. 1, pp 79–122, CRC Press, Inc., Boca Raton, FL.

Myers, A. G., Proteau, P. J., & Handel, T. M. (1988) Stereochemical assignment of neocarzinostatin chromophore. Structures of neocarzinostatin chromophore–methyl thioglycolate adducts, *J. Am. Chem. Soc. 110*, 7212–7214.

Napier, M. A., Holmquist, B., Strydom, D. J., & Goldberg, I. H. (1979) Neocarzinostatin: spectral characterization and separation of a non-protein, *Biochem. Biophys. Res. Commun. 89*, 635–642.

Newton, B. A. (1964) Mechanisms of action of phenanthridine and aminoquinaldine trypanocides, *Adv. Chemother. 1*, 35–83.

Otting, G., Widmer, H., Wagner, G., & Wüthrich, K. (1985) Origin of t_1 and t_2 ridges in 2D NMR spectra and procedures for suppression, *J. Magn. Reson. 66*, 187–193.

Piantini, U., Sørensen, O. W., & Ernst, R. R. (1982) Multiple quantum filters for elucidating NMR coupling networks, *J. Am. Chem. Soc. 104*, 6800–6801.

Pletnev, V. Z., Kuzin, A. P., Trakhanov, S. D., & Kostetsky, P. V. (1982) Three-dimensional structure of actinoxanthin. IV. A 2.5 Å resolution, *Biopolymers 21*, 287–300.

Remerowski, M. L., Glaser, S. J., Sieker, L. C., Samy, T. S. A., & Drobny, G. P. (1990) Sequential ^{1}H NMR assignments and secondary structure of apo-neocarzinostatin in solution, *Biochemistry 29*, 8401–8409.

Samy, T. S. A., et al. (1983) Primary structure of macromomycin, an antitumor antibiotic protein, *J. Biol. Chem. 258*, 183–191.

Seaman, A., & Woodbine, M. (1954) The antibacterial activity of phenanthridine compounds, *Br. J. Pharmacol. 9*, 265.

Shaka, A. J., & Freeman, R. (1983) Simplification of NMR spectra by filtration through multiple quantum coherence, *J. Magn. Reson. 51*, 169–173.

Sieker, L. C. (1981) X-ray diffraction analysis of the antitumor protein neocarzinostatin: results at 3.5 ångstrom resolution, Ph.D. Thesis, University of Washington, Seattle, WA.

Subramanian, E., Trotter, J., & Bugg, C. E. (1971) Crystal structure of ethidium bromide, *J. Cryst. Mol. Struct. 1*, 3–15.

Suzuki, H., Miura, K., Kumada, Y., Takeuchi, T., & Tanaka, N. (1980) Biological activities of nonprotein chromophores of antitumor protein antibiotics: suromomycin and neocarzinostatin, *Biochem. Biophys. Res. Commun. 94*, 255–261.

Takeshita, J., Maeda, H., & Koike, K. (1980) Subcellular action of neocarzinostatin: Intracellular incorporation, DNA breakdown and cytotoxicity, *J. Biochem. 88*, 1071–1080.

Takeshita, M., Kappen, L. S., Grollman, A. P., Eisenberg, M., & Goldberg, I. H. (1981) Strand scission of deoxyribonucleic acid by neocarzinostatin, auromomycin, and bleomycin: Studies on base release and nucleotide sequence specificity, *Biochemistry 20*, 7599–7606.

Tanaka, T., Hirama, M., Ueno, M., Imajo, S., Ishiguor, M., Mizugaki, M., Edo, K., & Komatsu, H. (1991) Proton NMR studies on the chromophore binding structure in neocazinostatin complex, *Tetrahedron Lett. 32*, 3175–3178.

Tanaka, T., Hirama, M., Fujita, K.-I., Imago, S., & Ishiguro, M. (1993) Solution structure of the antibiotic neocarzinostatin, a chromophore–protein complex, *J. Chem. Soc., Chem. Commun. 15*, 1205–1207.

Van Roey, P., & Beerman, T. A. (1989) Crystal structure analysis of auromomycin apoprotein (macromomycin) shows importance of protein side chains to chromophore binding selectivity, *Proc. Natl. Acad. Sci. U.S.A. 86*, 6587–6591.

Vilagines, R., & Atanasiu, P. (1967) Action of ethidium bromide on growth of herpes virus in cell cultures, *Nature 215*, 87–88.

Waring, M. J. (1964) Complex formation with DNA and inhibition of *Escherichia coli* RNA polymerase by ethidium bromide, *Biochim. Biophys. Acta 87*, 358–361.